

The Effect of Non-linear Pivot Stiffness on Tilting Pad Bearing Dynamic Force Coefficients

Ali ABASABADARAB*, SeyedAlireza HOSSEİNİ, Mohammad ABASABADARAB,

Reza ALLAHYARİ, Mahdi ESFAHANİATASHBEİK

M.Sc. of Mechanical Engineering, No19, East Gharmsar, South Shiraz St, Vanak Sq, Tehran

M.Sc. of Mechanical Engineering, Amirkabir University of Technology

Received: 01.02.2015; Accepted: 05.05.2015

Abstract. Journal bearings are used on a variety of different rotating and reciprocating machines to support shafts that are rotating inside a bearing. In contrast to anti-friction type bearings where the primary mechanism is rolling action of contacting components, journal bearings operate by supporting the load of the shaft on a pressurized oil film. Approach of this paper is to describe static and dynamic loads and dynamic characterizes that effect on fluid film thickness and enhance tilting pad bearing model by including nonlinear pivot flexibility for rocker, spherical, and flexure type pivots.

Keywords: Tilting pad, Dynamic, Pivot, Static, force coefficient

1. INTRODUCTION

Figure 1 show a tilting pad journal bearing comprised of four pads. Each pad tilts about its pivot making a hydrodynamic film that generates a pressure reacting to the static load applied on the spinning journal. This type of bearing is typically installed to carry a static load on a pad (LOP) or a static load in between pads (LBP). Commercial tilting pad bearings have various pivot designs such as rocker pivots (line contact), spherical pivots (point contact) and flexure supported pivots.

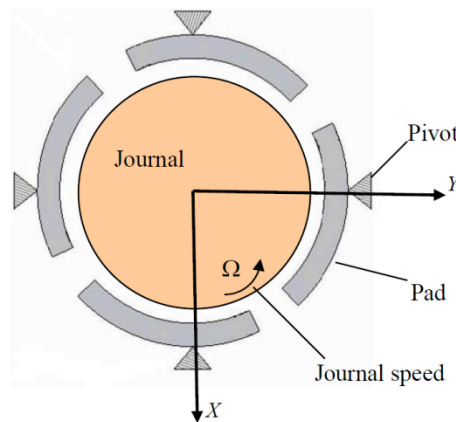


Figure1. Schematic views of a four pad tilting pad bearing [1].

*Corresponding author. *Email address: aabasabadi@pted-co.com*

Accurate prediction of tilting pad bearing forces and force coefficients is essential to design and predict the dynamic performance of rotor-bearing systems. Parameters affecting tilting pad bearing force coefficients include elastic deformation of the bearing pads and pivots, thermal effects affecting the lubricant viscosity and film clearance, etc. [2, 3].

Rocker and spherical pivots in tilting pad allow nearly frictionless pad rotation. An ideal rocker TPB, shown in Figure 3(a), allows the pad to roll without slipping around a cylindrical pivot inside the curvature of the bearing. A spherical TPB, seen in Figure 3(b), allows the pad to rotate about a spherical pivot fixed to the inside curvature of the bearing [4].

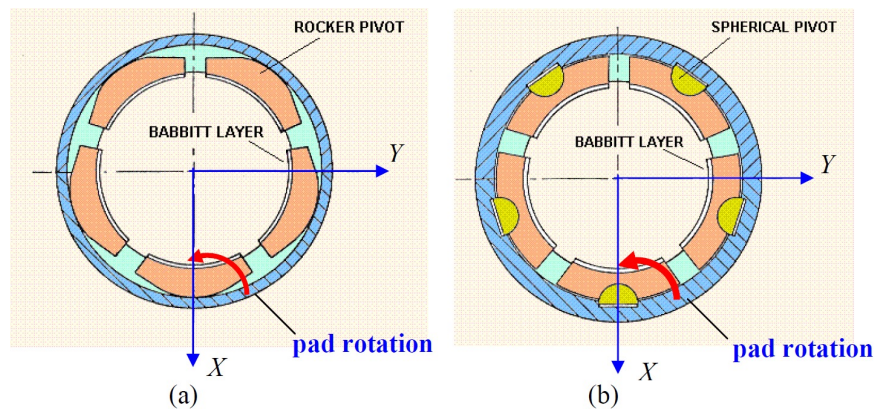


Figure 3. Rocker pivot (a) and spherical pivot (b) in a tilting pad journal bearing [5].

The flexure pivot TBP, depicted in Figure 4, is a modern advancement in TBP designs. It is a two piece configuration that uses electron discharge machining to manufacture the pad, connected by a flexure thin web to the bearing housing. This design eliminates tolerance stack ups that usually occur during manufacturing and assembly, pivot wear, and unloaded pad flutter problems which occur in conventional tilting pad bearings [4].

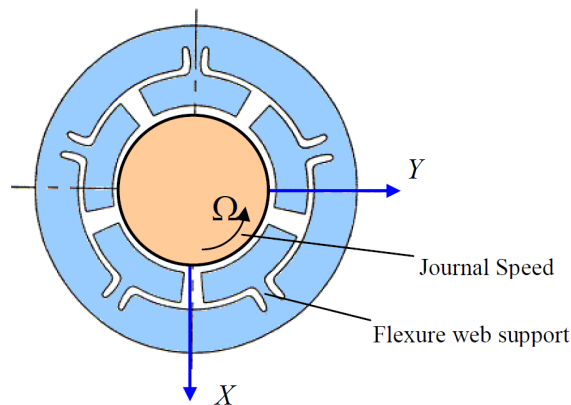


Figure 4. Schematic view of flexure pivot TPB [6].

As seen in Figure 5, pivot flexibility makes the pad to displace along the radial (ξ) and transverse (η) directions. The pad also tilts or rotates with angle (δ) [5, 6].

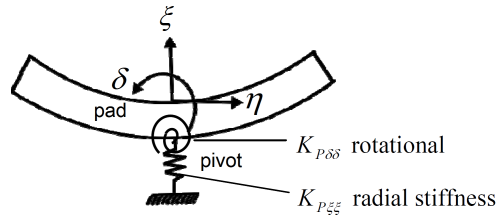


Figure 5. Displacement coordinates in a tilting pad with idealized depiction of pivot stiffness's [8].

2. ANALYSIS

2.1 Coordinate system and Fluid film thickness

Figure 6 shows the geometry and coordinate system for a tilting pad journal bearing. A local coordinate is placed on the bearing surface with the $\{x\}$ axis in the circumferential direction and the $\{z\}$ axis in the axial (in plane) direction. Inertial axes $\{X, Y, \text{ and } Z\}$ have origin at the bearing center. e_X, e_Y Represent the journal center displacements along the X, Y axes. The position of a tilting-pad is referenced to the angular coordinate $\theta = \frac{x}{R}$, with Θ_l as the pad leading edge angle, Θ_t as the pad trailing edge angle, and Θ_p as the pad pivot point angle. $(\delta^k, \xi^k, \eta^k)$ denote the k^{th} pad rotation and radial and transverse displacements; $k = 1, \dots, N_{pad}$. [7].

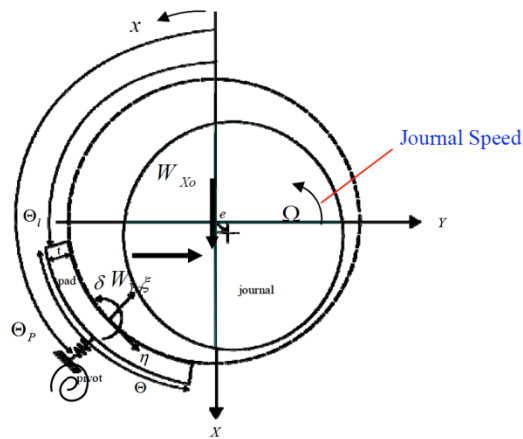


Figure 6. Geometry and nomenclature for a tilting pad with flexible pivot [8].

The fluid film thickness in the k_{th} pad is [8],

$$h = C_p + e_X \cos(\theta) + e_Y \sin(\theta) + (\xi^k - r_p) \cos(\theta - \Theta_p) + (\eta^k + R\delta^k) \sin(\theta - \Theta_p)$$

Where C_p is the pad machined radial clearance, and $r_p = C_p - C_m$ is the pad preload with C_m as the bearing assembled clearance. Presently, for simplicity, a bearing pad is assumed rigid [8].

3. PERTURBATION ANALYSIS

Duo to prepare an numerical analysis, Consider small amplitude journal and pad motions about static equilibrium position (SEP) and applying an external static load with components (W_{X0}, W_{Y0}) to the journal determines its static equilibrium position (e_{X0}, e_{Y0}) with fluid static pressure field $\{P_0^k\}$, film thickness $\{h_0^k\}$, and corresponding equilibrium k^{th} pad rotation and deflections $\{\delta_0^k, \xi_0^k, \eta_0^k\}$. Small amplitude journal center motions $(\Delta e_{X0}, \Delta e_{Y0})$ of frequency ω about the static equilibrium point. Hence:

$$e_X(t) = e_{X0} + \Delta e_X e^{i\omega t} \quad \text{and} \quad e_Y(t) = e_{Y0} + \Delta e_Y e^{i\omega t}$$

And for $k = 1, \dots, N_{pad}$, will have:

$$\delta^k(t) = \delta_0^k + \Delta \delta^k e^{i\omega t} \quad , \quad \xi^k(t) = \xi_0^k + \Delta \xi^k e^{i\omega t} \quad , \quad \eta^k(t) = \eta_0^k + \Delta \eta^k e^{i\omega t}$$

The sum of the pads fluid film reaction forces must balance the external load (W_X, W_Y) applied on the journal. The external forces add a static (equilibrium) (W_{X0}, W_{Y0}) load to a dynamic part $(\Delta W_X, \Delta W_Y) e^{i\omega t}$ [8].

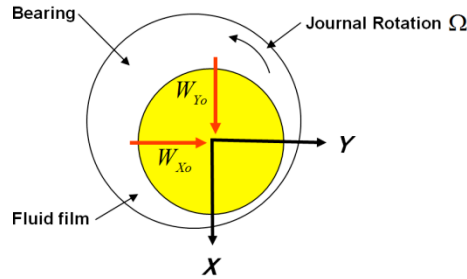


Figure 7. The external forces add a static (equilibrium) [8].

$$W_X = W_{X0} + \Delta W_X e^{i\omega t} = \sum_{k=1}^{N_{pad}} F_X^k \quad , \quad W_Y = W_{Y0} + \Delta W_Y e^{i\omega t} = \sum_{k=1}^{N_{pad}} F_Y^k$$

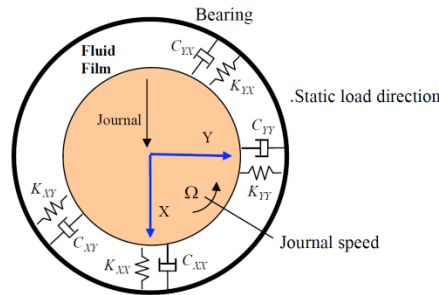


Figure 8. Conceptual depiction of stiffness and damping coefficients in a fluid film journal bearing [8].

The equations of motion for the k^{th} pad are:

$$[M_{pad}^k] \begin{Bmatrix} \Delta \ddot{\delta}^k \\ \Delta \ddot{\xi}^k \\ \Delta \ddot{\eta}^k \end{Bmatrix} = \begin{Bmatrix} M_p^k \\ F_{p\xi}^k \\ F_{p\eta}^k \end{Bmatrix} + \begin{Bmatrix} M^k \\ F_{\xi}^k \\ F_{\eta}^k \end{Bmatrix}$$

Where $M_p^k, F_{p\xi}^k, F_{p\eta}^k$ are the pad pivot reaction moment and forces, and $M^k, F_{\xi}^k, F_{\eta}^k$ are the fluid film forces acting on the k^{th} pad. The pad mass matrix is:

$$[M_{pad}^k] = \begin{bmatrix} I_p^k & m^k b^k & -m^k c^k \\ m^k b^k & m^k & 0 \\ -m^k c^k & 0 & m^k \end{bmatrix}$$

With b and c as the radial and transverse distances from the pad center of mass to the pad pivot, respectively. m^k and I_p^k are the pad mass and mass moment of inertia about the pad pivot. $I_p^k = I_G^k + m^k(c^2 + b^2)$, where is I_G^k the pad moment of inertia about its center of mass [9].

4. EVALUATION of PIVOT NONLINEAR STIFFNESS

The pivot stiffness is, in general, a nonlinear function of the applied (fluid film) load acting on a pad. Consider, as sketched in Figure 7, a typical radial force $F_{p\xi}$ versus pivot nonlinear radial deflection (ξ) [9].

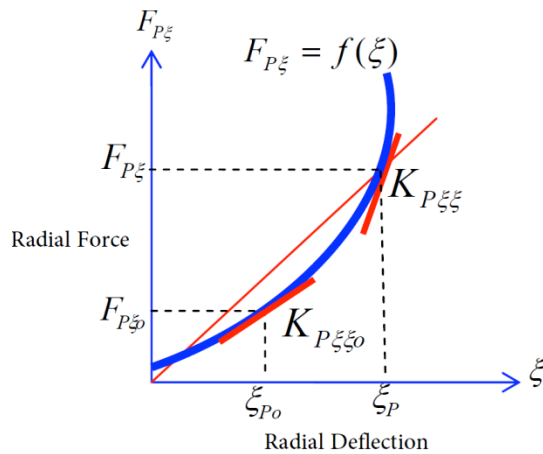


Figure 9. Typical force versus pivot (nonlinear) radial deflection [9].

The assumption of small amplitude motions about an equilibrium position allows the pivot reaction radial force to be expressed as:

$$F_{P\zeta} = F_{P\zeta_0} + K_{P\zeta_0} \Delta\zeta_P$$

Where $F_{P\zeta} = f(\zeta_{P0})$ is the static load on the pivot and $K_{P\zeta_0} \Delta\zeta_P$ is the force due to radial displacement. [9]

5. COMPARISON between PREDICTED STATIC and DYNAMIC COEFFICIENTS and REF. [10]

Figure 9 depicts a schematic view of a five pad, rocker back, TPB tested by Carter and Childs [10]. Bearing force coefficients were experimentally obtained for shaft speeds from 4k-12k rpm and static loads from 0 -19.5 kN. [10].

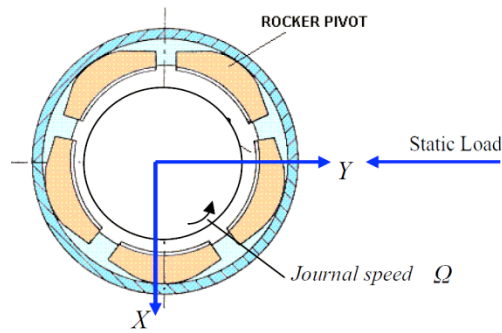


Figure10. Five pad tilting pad bearing [10].

Mineral oil (Mobil DTE) ISO VG32 lubricated the bearing. The lubricant inlet supply pressure and temperature are 1.55 bar (gauge) and 43° C, respectively. The load applied to the bearing is along the -Y direction. Table 1 details the bearing geometry and fluid properties.

Table 1. Test bearing geometry and operating conditions [10].

Geometry, Operation and condition	Value	Fluid Properties, Ref. [10]	Mobile DTE ISO VG32
Rotor diameter, D	101.587 mm	Viscosity @ 40° C	31 cSt
Pad axial length, L	60.32 mm	Viscosity @ 100° C	5.5 cSt
Pad number and arc length	5(57.87°)	Density @ 15°C	850 kg/m ³
Pivot offset	60%	Specific heat	1951 J/(kg-K)
Loaded radial pad clearance, C _p	110.5 mm		
Loaded radial bearing clearance, C _b	79.2 mm		
Pad preload, $r_p = 1 - \frac{C_b}{C_p}$	0.283		
Pad mass, m _p	1.0375 kg		
Pad mass moment of inertia (at pivot), I _p	0.00045 kg-m ²		

For load-between-pad configuration (LBP), Carter and Childs [10] present nonsynchronous force coefficients versus load. Figure 10 shows Ref. [10] predicted and experimental direct

stiffness's for a journal speed of 4000 rpm. Experimental direct stiffness K_{yy} is over predicted by ~28% for a static load of 14.8 kN [10].

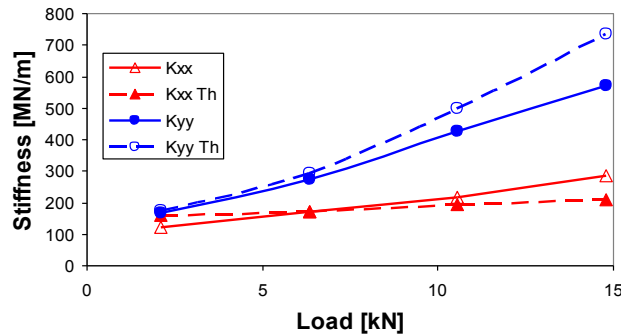


Figure 11. Predicted and experimental direct stiffness for operation shaft speed of 4000 rpm [10].

Figure 12 shows the predicted direct static force coefficients versus static load given a flexible rocker pivot and a rigid pivot for an isothermal flow case. The direct static stiffness's decrease for a flexible pivot, the difference amounting to a large percentage, ~ 33% [10].

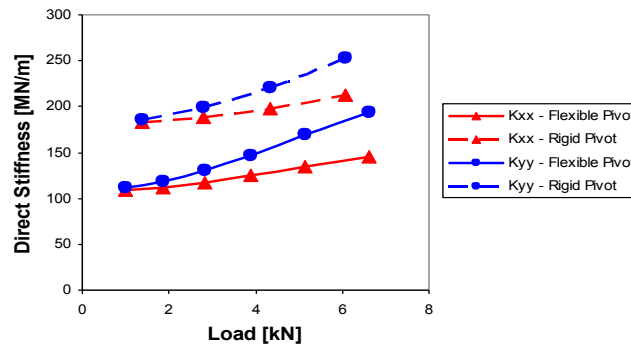


Figure 12. Predicted static direct stiffness's versus static load [10].

Figure 13 shows the predicted bearing static eccentricity versus applied load when considering both a rigid pivot and a flexible pivot.

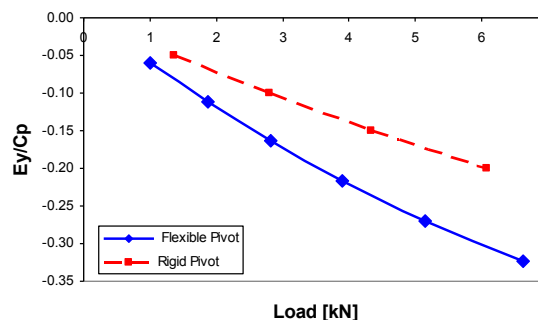


Figure 13. Predicted bearing static eccentricity versus static load (-Y direction) [10].

6. CONCLUSION

This paper introduces a general framework to identify linear and nonlinear stiffness and damping coefficients on journal bearings. The article describe static and dynamic loads and dynamic characterizes that effect on fluid film thickness and enhance tilting pad bearing model by including nonlinear pivot flexibility for rocker, spherical, and flexure type pivots. Result show that an improvement in bearing force coefficient predictions is when pivot stiffness is placed in series with the bearing force coefficients derived from a rigid pivot model.

REFERENCES

- [1] Harris, J., and Childs, D., 2008, "Static Performance Characteristics and Rotor dynamic Coefficients for a Four-Pad Ball-In-Socket Tilting Pad Journal Bearing," ASME Paper No. GT2008-5063.
- [2] San Andrés, L., 1996, "Turbulent Flow, Flexure-pivot Hybrid Bearings for Cryogenic Applications," ASME J. Tribol., 118(1), pp. 190-200.
- [3] Kim, J., Palazzolo, A., and Gadangi, R., 1995, "Dynamic Characteristics of TEHD Tilt Pad Journal Bearing Simulation Including Multiple Mode Pad Flexibility Model," ASME J. Vib. Acoustics, 117, pp. 123-135.
- [4] Lund, J. W., 1964, "Spring and Damping Coefficients for the Tilting-Pad Journal Bearing," ASLE Trans., 7, 4, pp. 342-352.
- [5] Hagg, A. C., and Sankey, G. O., 1958, "Some Dynamic Properties of Oil-Film Journal Bearings with Reference to the Unbalance Vibration of Rotors," ASME J. Appl. Mech., 25, 141.
- [6] Rouch, K. E., 1983, "Dynamics of Pivoted-Pad Journal Bearings, Including Pad Translation and Rotation Effects," ASLE Trans., 26, 1, pp. 102-109.
- [7] Kirk, R. G., and Reedy, S. W., 1988, "Evaluation of Pivot Stiffness for Typical Tilting-Pad Journal Bearing Designs," J. Vib., Acoustics, Stress, and Reliability in Design, 110, pp. 165-171.
- [8] Carter, R. C., and Childs, D., 2008, "Measurements Versus Predictions for the Rotor dynamic Characteristics of a 5-Pad, Rocker-Pivot, Tilting-Pad Bearing in Load between Pad Configuration," ASME Paper No. GT2008-5069.
- [9] "Tilting Pad Journal Bearings," Rotech Engineering, [accessed 10 April 2008]
- [10] Zeidan, F.Y., 1992, "Developments in Fluid Film Bearing Technology," Turbo machinery International, 9, pp. 24-31.